

Extraction of Graphene-Titanium Contact Resistances using Transfer Length Measurement and a Curve-Fit Method

Johanna Anteroine, Wonjae Kim, Kari Stadius, Juha Riikonen, Harri Lipsanen, Jussi Ryyänen

Abstract—Graphene-metal contact resistance limits the performance of graphene-based electrical devices. In this work, we have fabricated both graphene field-effect transistors (GFET) and transfer length measurement (TLM) test devices with titanium contacts. The purpose of this work is to compare the contact resistances that can be numerically extracted from the GFETs and measured from the TLM structures. We also provide a brief review of the work done in the field to solve the contact resistance problem.

Keywords—Contact resistance, graphene, TLM

I. INTRODUCTION

GRAPHENE is a hexagonally-organized form of carbon atoms that is only one atomic layer thick [1]. It is the thinnest material known to man so far, and the atomic structure gives rise to exceptional electrical, optical, mechanical and thermal properties [2]. The most interesting electrical properties are high electron mobility and ballistic transport of charge carriers.

Graphene field-effect transistors utilize mono- or few-layer graphene as channel material. Graphene displays an ambipolar field effect that can be explained with the bandstructure [1]. An applied electric field induces doping in graphene by changing the Fermi energy which is an effect often referred to as self-doping. Self-doping allows the charge carrier type and concentration to be controlled with an outside electric field, or rather with a gate voltage. Graphene is a semimetal which means that it has no band gap. This results in poor on/off ratio for current. The lack of a band gap in intrinsic graphene is, together with large scale manufacturing, one of the most challenging problems for electronics. Having no band gap is a problem if graphene is to be used in logic circuits in much the same way as silicon is used today as the material for CMOS logic circuits [3]. Nonetheless, there are applications where the trade-off between high power consumption and high performance is negotiable. One such example is radio frequency (RF) applications.

Although, GFETs show promise for RF applications, there is one obstacle in the way, the graphene-metal contact resistance. The contact resistance of the metal-graphene junction should be as small as possible. Reducing contact resistance is crucial especially in GFETs with very a short channel, because high contact resistance may otherwise limit the operation by lowering the cut-off frequency. The contact resistance of

Authors are with the Department of Micro- and Nanosciences, Aalto University School of Electrical Engineering, 02150 Espoo, Finland e-mail: johanna.anteroinen@aalto.fi.



Fig. 1. Two transfer length measurement test structures each with 5 contact pads.

graphene/metal interface has not received much attention, and results are sometimes contradictory. For example, Venugopal et al. [4] propose that contact resistance is independent of gate voltage, whereas many others have observed that contact resistance does depend on the gate voltage [5]–[7].

In this paper, we have fabricated and measured GFETs and TLM test devices to investigate the graphene-titanium contact in room temperature. Moreover, we have compared the numerical curve-fitting method and the TLM measurement results to investigate the accuracy of a curve-fit method for circuit design modelling purposes. In Section II, the formation of the metal-graphene junction is discussed and background information is given. The measurement methods are explained in Section III and in Section IV, we discuss the results. Section V concludes the paper.

II. GRAPHENE CONTACT RESISTANCE

The intrinsic performance of graphene transistors is masked by the high contact resistance. Contact resistance is currently the major electric current limiting factor in GFETs [4]. The contact resistance limits the cut-off frequency, the transconductance and the current-gate voltage linearity of field-effect transistors.

The contact resistance, R_c , can be defined as the sum of the resistances of the physical metal interconnects, the metal-graphene interface (interfacial resistivity) and the ungated channel between contact and the transistor (access resistance). The contact resistance in a graphene transistor is illustrated in Fig. 2. The parasitic contact resistances are in series with the graphene channel resistance. As the specific contact resistivity is a combination of several phenomena, such as interfacial

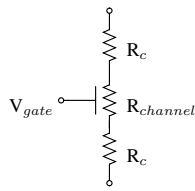


Fig. 2. Conceptual DC-model of a GFET.

resistivity, it cannot be predicted from theory. Theory is able to predict interfacial resistivity, which unfortunately cannot be measured directly [8].

The collected contact resistances from the recent articles are shown in Table I. Table I shows that there is a large variation between the contact resistances. Several studies show that graphene/metal R_c depends on the gate voltage with a maximum value at low gate voltages and minimum at high gate voltages [5]–[7]. The contact resistance in graphene/metal contacts is found to be dominated by a gate voltage independent part. The most probable explanation currently offered, is due to significant charge transfer at the graphene/metal interface shifting the Fermi level of the graphene far away from degeneracy point [7]. It is suggested that only the top layers in a graphene stack contribute to contact formation [4] [5]. The gate voltage independent part of R_c has been found to correlate with the background pressure during processing with lower pressure resulting in lower R_c [7]. This is believed to be related to adsorption of molecules prior to evaporation or the oxidation of the metal layer during deposition.

The current flow path at graphene/metal contact is through the edge i.e. current crowding takes place at the edge of the contact [5]. The transition from edge conduction to area conduction takes place for a contact length shorter than the transfer length $1 \mu\text{m}$ for Ni/graphene contact [5]. Transfer length is a quantity describing the distance over which most of the current ($1/e$) is transferred from the semiconductor to the metal or vice versa. The transfer length is described as

$$L_T = \sqrt{\frac{\rho_c}{R_{sh}}} \quad (1)$$

where ρ_c is the specific contact resistivity and R_{sh} is the sheet resistance of graphene [8]. Transfer length is a property of the system and is dependent on which metal is used.

More importantly, the recent studies show that the choice of contact metal is crucial for the device performance. Table II shows the work functions for several metals. It has been observed experimentally that high work function difference between graphene and the metal results in lower contact resistance [5]. Typically a great difference between metal/semiconductor work functions predict a high contact resistance. It is understood that for the case of a large difference in work functions, the electron is transferred from metal to graphene increasing the density of states in graphene under the metal contact and thus reducing the specific contact resistance [5].

One practical model of GFET total device resistance presented by Kim et al. [10]. The model describes the total device resistance as a function of top gate voltage (V_{TG}) and consists

TABLE I
COLLECTED CONTACT RESISTIVITY VALUES (T = 300 K).

Metal/Graphene	ρ_c	References
Pd	$\sim 230 \Omega \mu\text{m}$	[6]
Ni	$500 \Omega \mu\text{m}$	[5]
Ti	$> 1000 \Omega \mu\text{m}$	[5]
Ti	$< 250 \Omega \mu\text{m}$ (liquid helium temp.)	[9]

TABLE II
THE WORK FUNCTIONS OF SEVERAL METALS.

Metal	Ni	Ti	Graphene	Cr	Pd
ϕ	5.2 eV	4.3 eV	4.5 eV	4.6 eV	5.22-5.6 eV

of three equations:

$$n_{tot} = \sqrt{n_0^2 + n[(V_{TG} - V_{DRC})]^2} \quad (2)$$

$$V_{TG} - V_{DRC} = \frac{qn}{C_{ox}} + \frac{\hbar v_F \sqrt{\pi n}}{q} \quad (3)$$

$$\hat{R} = R_c + R_{channel} = R_c + \frac{N_{sq}}{n_{tot} q \mu} \quad (4)$$

where n_{tot} is the charge carrier concentration, q is the elementary charge, μ is the conductivity mobility, v_F is the Fermi velocity in graphene, C_{ox} is the oxide layer capacitance, \hat{R} is the predicted total device resistance, R_c is the contact resistance and N_{sq} is the number of squares. Eq. (2)-(4) allows an estimate of the contact resistance from a single current-voltage measurement, even though the effect of gate voltage on R_c is neglected here.

III. MEASUREMENT METHODS

Measuring contact resistance is complicated though the measurement itself is often simple. Different measurement strategies may easily lead to very different results and the interpretation of the results is complicated [8]. A well-known method to directly measure R_c is the transfer length method (TLM) that should not be confused with transmission line model (also abbreviated TLM) used to characterize semiconductor sheet resistance and R_c [8]. Both methods use a similar test device geometry, but transfer length method has more than three contacts. A schematic of the transfer length method test device is shown in Fig. 3 and a close-up of one actual device is shown in Fig. 1. There are altogether four test structures in the die we fabricated. The distances between contacts are 1, 2, 4 and $8 \mu\text{m}$ and the width, W , of each contact is $10 \mu\text{m}$ and the length, L , of the contact is $1 \mu\text{m}$. Transfer length measurement is performed so that the total resistance is measured between adjacent contacts, e.g. in Fig. 3 the resistance is measured between A-D, D-B, B-E, E-C and C-F.

Another method to acquire R_c is to extract the R_c from total device resistance of a GFET by using Eq. (2)-(4). The total resistance is measured against the back or top gate voltage. This method was suggested in [4] and [10], though the former

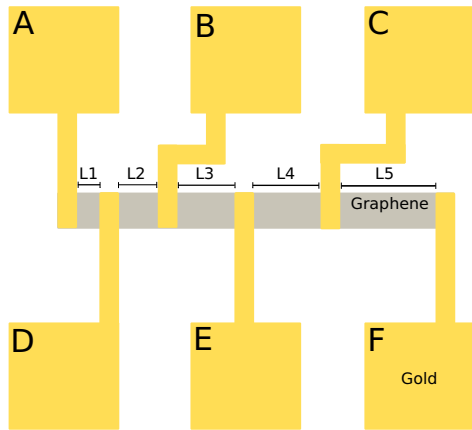


Fig. 3. Transfer length measurement principle.

reference provides validation of the suggested method with transfer length measurement. Equations (2)-(4) can be used to extract contact resistance from a single measurement through curve-fitting. Similarly, according to [4], R_c can be retrieved from $V_{TG} - R_{Total}$ -curve in the high gate voltage limit. A rough estimate of R_c is the 'tail' of the total resistance curve at the high voltage limit.

IV. RESULTS

The measured total device resistances are plotted against the contact spacings in Fig. 4. Contact resistance is the extrapolated value of resistance at zero distance. TLM gives the sheet resistance, the contact resistance and the specific contact resistivity. The TLM measurement results were fitted according to Eq. (5).

$$R_T = \frac{R_{sh}d}{W} + 2R_c \approx \frac{R_{sh}}{W}(d + 2L_T) \quad (5)$$

where d is the distance between contacts.

Fig. 4 shows the TLM measurement results with the 1st order polynomial fit. The $2R_c$ value is found in Fig. 4 at $L = 0 \mu\text{m}$, and the $2L_T$ value is found at $R = 0$. The slope in Fig. 4 gives the R_{sh}/W -value. Table III shows that the difference in R_c is quite significant between different test structures. The TLM structures number 3 and 4 had three measurement points instead of four, because the fabrication of the last contact length, $8 \mu\text{m}$, was failed in both devices. The results show that in two of the TLM devices the $L_T > L$, which would indicate that the contacts may have been too short for accurate measurement. The results in Table III are in the same range as the state-of-the-art.

The model described by Equations (2)-(4) was fit to the VI-measurement data of four GFETs of the same size and one different size GFET with nonlinear least squares curve fitting algorithm in Matlab. Optimization algorithm finds parameters that minimize the following cost function

$$J(x) = \sum_i (\hat{R}(x, V_{TG,i}) - R(V_{TG,i}))^2 \quad (6)$$

where x is a vector containing the three unknown parameters: contact resistance R_c , residual carrier density n_0 and mobility

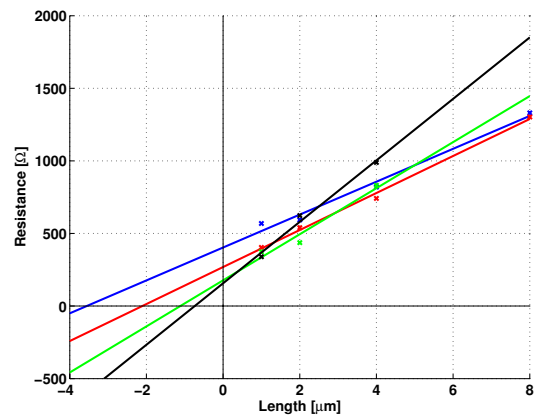


Fig. 4. TLM measurement results.

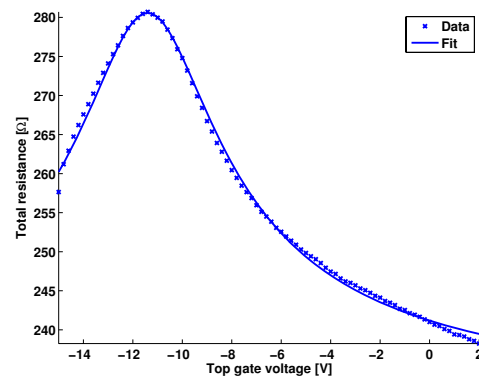


Fig. 5. GFET with dimension $W=25 \mu\text{m}$ and $L=0.5 \mu\text{m}$. This image corresponds to the first row in Table IV. The back gate voltage is 0V.

μ . $\hat{R}(x, V_{TG,i})$ is the total device resistance predicted by the model with parameters x and applied top-gate voltage $V_{TG,i}$. The actual measured resistances are denoted with $R(V_{TG,i})$. The operation of the curve-fit algorithm was evaluated with k-fold cross-validation with ten folds and three repetitions [11].

Fig. 5 shows the curve-fit results for a GFET with $W=25 \mu\text{m}$ and $L=0.5 \mu\text{m}$. Table IV shows the curve-fit results for GFETs. The variation in the GFET properties is evident in Table IV. The GFET with the lowest value of R_c in Table IV has the highest mobility, as is expected.

The contact resistance values from the curve-fit algorithm were normalized to be comparable to the TLM measurement. It was assumed that the drain contact has much larger contact resistance, and the contact area was determined by the drain contact. The results of the curve-fit after the normalization are smaller than expected. This is due to the underestimation of the actual contact area. For GFETs, the access resistance is expected to be larger than in the TLM devices due to the different geometry of the device. Also, the curve-fit neglects that the contact resistance depends on the gate voltage. To improve R_c , the first steps should be to improve the quality of the graphene layer and investigate different metallization schemes.

TABLE III
MEASURED AND CALCULATED VALUES OF THE TLM STRUCTURES.

TLM	R_c [Ω]	R_c/A [Ω/cm^2]	$R_c/(2l + 2W)$ [$\Omega/\mu m$]	R_{sh}/W [$\Omega\text{-sq}$]	L_T [μm]
1	201.5	$2.0 \cdot 10^9$	9.2	113.3	1.8
2	133.5	$1.3 \cdot 10^9$	6.1	127.5	1.1
3	88.5	$8.8 \cdot 10^8$	4.0	158.7	0.6
4	78.5	$7.8 \cdot 10^8$	3.6	211.7	0.4

TABLE IV
CURVE-FIT EXTRACTION RESULTS FOR FOUR GFETs WITH $W/L = 25/0.5 \mu m$. THE RESULTS FOR A GFET WITH $W=50\mu m$ AND $L=1 \mu m$ IS SHOWN ON THE LAST ROW.

W/L	R_c [Ω]	R_c/A [Ω/cm^2]	$R_c/(2l + 2W)$ [$\Omega/\mu m$]	$n_0 \cdot 10^{12}$ [cm^{-2}]	μ [cm^2/Vs]
25/0.5	116.3	$9.7 \cdot 10^7$	3.6	5.9	405.1
25/0.5	57.3	$4.6 \cdot 10^7$	3.8	5.4	446.6
25/0.5	274.0	$2.2 \cdot 10^8$	4.6	7.6	235.5
25/0.5	234.7	$1.9 \cdot 10^8$	3.9	5.1	419.1
50/1	140.4	$5.6 \cdot 10^8$	1.3	4.8	289.8

V. CONCLUSION

The operation of GFETs is limited by the low current on/off ratio and high contact resistance, as well as the defects and impurities in the graphene. Graphene-metal contact resistance has gradually gained more attention, and experimental results have been published. Yet, comprehensive theoretical explanations of the graphene-metal contact resistance are still missing. Moreover, predicting the contact resistance of any graphene-based device is currently missing.

The contact resistance of graphene-titanium-contact was investigated in this work using two methods, the transfer length method and a curve-fit method. The transfer length method requires separate devices to be fabricated. The curve-fit method applies for micrometer-size GFETs and does not require additional measurements or devices. Both methods give insight to the graphene-metal contact resistance, and as is to be expected, give different results for the contact resistance. For GFET circuit level modelling and design, the curve-fit method is practical, quick and gives a good estimation of the contact resistance. The contact resistance values from the transfer length measurement are in line with the state-of-the-art, yet for practical applications the GFET contact resistance needs to be improved.

ACKNOWLEDGMENT

The research leading to these results has received funding from the European Community's Seventh Framework Programme (FP7/2007-2013) under grant agreement no 246026.

REFERENCES

[1] K. S. Novoselov, A. K. Geim, S. V. Morozov, D. Jiang, Y. Zhang, S. V. Dubonos, I. V. Grigorieva, and A. A. Firsov, "Electric Field Effect in Atomically Thin Carbon Films," *Science*, vol. 306, no. 5696, pp. 666-669, 2004. [Online]. Available: <http://www.sciencemag.org/cgi/content/abstract/306/5696/666>

[2] A. K. Geim and K. Novoselov, "The Rise of Graphene," *Nature Materials*, vol. 6, pp. 183-191, 2007. [Online]. Available: <http://dx.doi.org/10.1038/nmat1849>

[3] F. Schwierz, "Graphene transistors," *Nature Nanotechnology*, vol. 5, pp. 487-496, 2010. [Online]. Available: <http://dx.doi.org/10.1038/nnano.2010.89>

[4] A. Venugopal, L. Colombo, and E. M. Vogel, "Contact resistance in few and multilayer graphene devices," *Applied Physics Letters*, vol. 96, no. 1, p. 013512, 2010. [Online]. Available: <http://link.aip.org/link/?APL/96/013512/1>

[5] K. Nagashio, T. Nishimura, K. Kita, and K. Toriumi, "Contact resistivity and current flow path at metal/graphene contact," *Applied Physics Letters*, vol. 97, no. 14, p. 143514, 2010. [Online]. Available: <http://link.aip.org/link/?APL/97/143514/1>

[6] F. Xia, V. Perebeinos, Y.-M. Lin, Y. Wu, and P. Avouris, "The origins and limits of metal-graphene junction resistance," *Nature Nanotechnology*, vol. 6, pp. 179-184, 2011. [Online]. Available: <http://dx.doi.org/10.1038/nnano.2011.6>

[7] S. Russo, M. Craciun, M. Yamamoto, A. Morpurgo, and S. Tarucha, "Contact resistance in graphene-based devices," *Physica E: Low-dimensional Systems and Nanostructures*, vol. 42, no. 4, pp. 677 - 679, 2010, 18th International Conference on Electron Properties of Two-Dimensional Systems. [Online]. Available: <http://www.sciencedirect.com/science/article/pii/S1386947709005165>

[8] D. Schroder, *Semiconductor Material and Device Characterization*. Wiley, 2006.

[9] R. Danneau, F. Wu, M. F. Craciun, S. Russo, M. Y. Tomi, J. Salmilehto, A. F. Morpurgo, and P. J. Hakonen, "Shot noise in ballistic graphene," *Phys. Rev. Lett.*, vol. 100, p. 196802, May 2008. [Online]. Available: <http://link.aps.org/doi/10.1103/PhysRevLett.100.196802>

[10] S. Kim, J. Nah, I. Jo, D. Shahrjerdi, L. Colombo, Z. Yao, E. Tutuc, and S. K. Banerjee, "Realization of a high mobility dual-gated graphene field-effect transistor with Al_2O_3 dielectric," *Applied Physics Letters*, vol. 94, no. 6, p. 062107, 2009. [Online]. Available: <http://link.aip.org/link/?APL/94/062107/1>

[11] E. Alpaydin, *Introduction to Machine Learning*. The MIT Press, 2004.